Modeling alternative tapering schemes for electron-positron Future Circular Collider (FCC-ee)

Milica Rakić
milica.rakic@epfl.ch

Mentor: Dr. Tatiana Pieloni

June 11, 2021

Travaux Pratiques 4 (TPIV) report

Contents

1 Introduction **2**

2 Tapering **2**
2.1 Basic concepts 2
2.2 Perfect/Individual tapering 4
2.3 Average tapering 5

3 Results **6**

4 Conclusion **13**

References **13**

1 Introduction

The FCC is a future hadron and lepton circular collider, designed to breach the limit of detection for heavy particles. More specifically FCC-ee electron positron collider is designed to detect Z, W, Higgs bosons and the top quark, thus, giving a basis for further Standard Model testing. This collider is designed of two rings that allow for a large number of bunches, with the circumference of around 100 km and the crossing angle of 30 mrad that allows for low beta function at interaction point (IP) and high beam-beam tune shift.

A limitation for any lepton circular collider is the synchrotron radiation, which causes energy loss and changes the trajectories of beam particles. Energy loss is compensated by the radio frequency (RF) cavities. However, these combined with any errors within magnets will produce periodic local deviation from the nominal beam energy E_0. Consequently, the deviation will influence particle orbits, potentially ending in resonances and beam loss. For these reasons, the introduction of a tapering scheme is of critical importance.

Therefore, during this TPIV, the effect of various tapering schemes on beam orbits and optics for the Higgs physics FCC-ee lattice have been looked into. Furthermore, a prototype of an average tapering scheme has been developed. For this purpose, acceleration toolbox (AT) software - a collection of tools used to model storage rings and beam transport in MatLab - and its python implementation pyAT have been used.[1]

/	Z	WW	ZH	TT
E [GeV]	45.6	80	120	175/182.5
ΔE [GeV]	0.036	0.34	1.72	7.8/9.2

Table 1: Initial beam energy E and energy loss per turn ΔE for Z, WW, ZH and TT physics lattices.

2 Tapering

2.1 Basic concepts

As introduced before, and can be seen in Table 1, the energy loss per turn in the FCC-ee due to radiation losses is very large, and is the most prominent for the high energy lattices. Consequently, particle energies will differ from the nominal beam energy. When such particles pass through dipoles, due to their difference in energy, they will be bent by different angles α:

$$\alpha = \frac{lBc}{E} \tag{1}$$

where l is the dipole arclength, B is the magnetic field and E is the particle energy. Expressed in the terms of nominal bending angle α_0, we can further stress the energy dependence as:

1. The code is open source and can be found on GitHub.

$$\alpha = \alpha_0 \left(1 - \frac{\Delta E}{E_0}\right) \tag{2}$$

Therefore, the orbit amplitude, as expressed in terms of a local dispersion $D(s)$, is:

$$x(s) = D(s)\frac{\Delta E}{E_0} \tag{3}$$

This results in particles being forced on different trajectories, as shown in Figure 1. Consequence of such behaviour is the creation of a so-called sawtooth-orbit. This effect for the FCC-ee lattice is shown in the blue plot in Figure 3. It can be seen that the x coordinate will periodically oscillate and can reach values of 0.6 mm. To reduce optics distortions, it would be preferential to decrease this value to at least 0.1 mm[2]. By adjusting the local dipole field there is a possibility to correct for particle deviations, shown in Figure 2.[3]

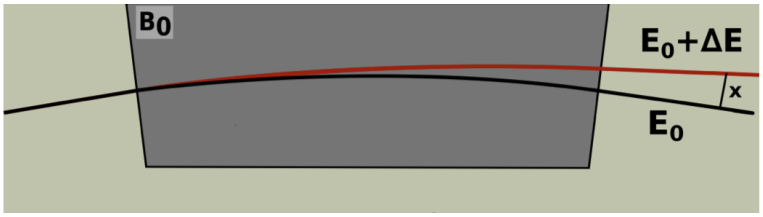

Figure 1: Dipole before tapering. A particle with an energy deviation ΔE is forced away from the ideal orbit.[4]

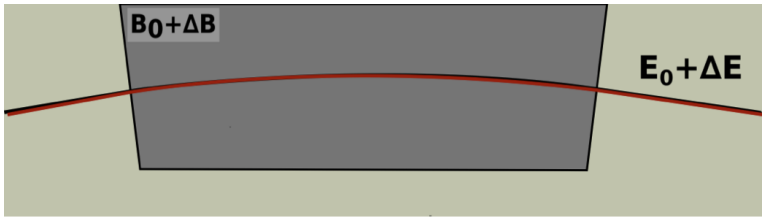

Figure 2: Dipole after tapering. A particle with an energy deviation ΔE now moves on the ideal orbit.[5]

Tapering is a concept of locally adjusting the dipole magnet strengths to compensate for beam energy loss. Such adjustment can be applied to every magnet individually (which is an expensive but best option) and to a set of magnets which are given an averaged tapering strength (more economical).

2. K.Oide, personal communication.

3. Bastian Härer, Andreas Doblhammer, and Bernhard Holzer, "Tapering Options and Emittance Fine Tuning for the FCC-ee Collider," in *7th International Particle Accelerator Conference* (June 2016), https://doi.org/10.18429/JACoW-IPAC2016-THPOR003.

2.2 Perfect/Individual tapering

The aforementioned sawtooth-orbit can be corrected by individually adjusting the strength of every dipole. Because reduced beam energy will result in increased focusing strength and therefore in optics distortions, the quadrupole, and sextupole fields need to be adjusted to the local energy as well.

The result of perfect tapering is shown in Figure 3, where the blue plot shows the orbit with no tapering included, and the orange plot after tapering is performed. The orbit amplitude is significantly decreased with individual tapering. It is important to note that the result of tapering is that the final lattice would have the same optics as in the case when no radiation is included.

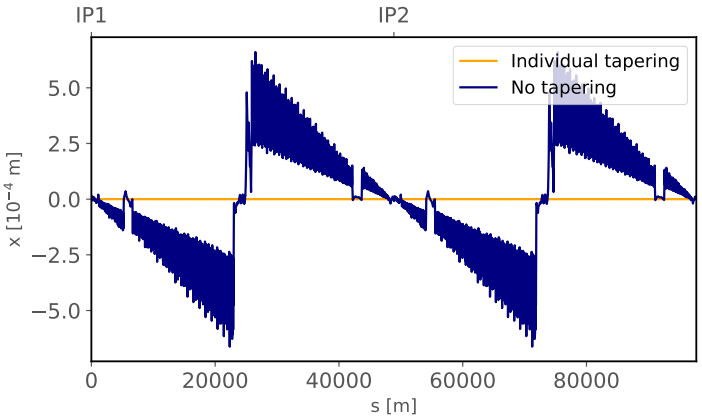

Figure 3: Sawtooth orbit for Higgs lattice in FCC-ee, shown in blue. Corrected orbit after perfect tapering is shown in orange.

However, even though the results obtained are promising, one problem remains, being the scale of the FCC machine. With the circumference of approximately 100 km, singularly adjusting the strength of every single dipole on the ring is both a financial and hardware challenge. Therefore, it is necessary to look into alternative tapering schemes to reduce the number of power supplies needed for the tapering.

2.3 Average tapering

Instead of perfectly tapering the whole lattice, an alternative scheme where a set of dipoles would obtain the same strength correction - average tapering - and thus require only a single common power supply, has been developed. The algorithm implemented is as follows:

1. The lattice dipoles are divided into a certain number of families with their subfamilies,
2. Perfect tapering is performed and results for dipole strength adjustments are recorded (values for PolynomB)
3. These results are factorised for every dipole within the given subfamily as:

$$f = \frac{k_p}{k_0} \tag{4}$$

   where k_p is the dipole strength after perfect tapering and $k_0 = \frac{\theta_d}{l_d}$ is the initial dipole strength as defined by the geometry; θ_d being dipole bending angle and l_d dipole length.
4. These factors f are averaged over the whole subfamily and applied back as averaged dipole strengths: $k_{av} = f \cdot k_0$.

While addressing the matter of dividing dipoles into families and subfamilies, there was above all a need to identify 'natural' dipole groupings within the lattice. Owning to the information supplied by K. Oide, the three most important lattice families were recognised: main arc dipoles at sextupole-free sections B1, main arc dipoles at long sextupole sections B1L and main arc dipoles at short sextupole sections B1S. These three families were further divided to receive an average tapering, while all other dipoles (e.g. dispersion suppressors, connecting arc, IP upstream and downstream) received perfect tapering.

Following the work done by Holzer, Doblhammer and Bastian[6], the B1, B1S and B1L dipoles were divided into four groups separated by the position of interaction points (IPs) and radio-frequency cavities (RFs). In other words, group one included all dipoles from the first IP to the first RF section, group two from the end of first RF section to the beginning of the second IP and so on. Thereafter, these four groups were additionally divided into a number N of subfamilies. The diagram of the above-mentioned division scheme is shown in Figure 4.

6. Härer, Doblhammer, and Holzer, "Tapering Options and Emittance Fine Tuning for the FCC-ee Collider."

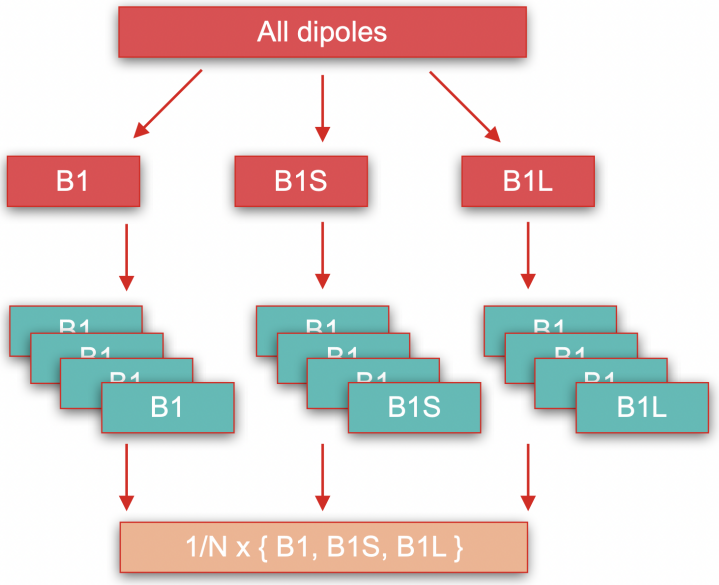

Figure 4: Division scheme of dipoles into families and subfamilies for the need of average tapering.

3 Results

The results of the average tapering scheme described in the last chapter are shown in this section. Three distinct family segmentations are presented, corresponding to 50, 100 and 200-micron orbit sizes. Exact values for emittances and optics for these three cases are shown in Table 2. The values are presented for only IP1 and IP2 as first figures of merit for luminosity predictions.

Table 2 shows that the emittance is reduced in the 50 micron case average tapering as compared to the individual tapering scheme. Furthermore, a small deviation in beta-functions at the IPs is observed pointing to a slight deterioration of the optics. With the increase of orbit to larger amplitudes (100 and 200-micron cases), the optics distortions become more significant. Moreover, the results for 100 micron orbit show that the emittance and dispersion experience a drastic change, and then return to some more expected values for 200 micron orbit. The potential reason why this is happening is that the subfamily segmentation is breaking the symmetry of sextupole pairs, and producing beam blowup. However, more careful examination of this result is needed.

Figure 5 shows the orbit (red plot) for half-arc splitting to around 100 sections, which corresponds to approximately eight B1, five B1S, and two B1L dipoles per subfamily. It can be seen that with this very fine splitting, the very well orbit of around 50 micron amplitude can be reproduced. The relative beta function and dispersion for this case are shown in Figure 6 and Figure 7. A deterioration of the optics is observed with respect to the perfect tapering scheme. Furthermore, this deterioration appears to exhibit a periodicity with a

periodic length of the half the length of the accelerator. The reasoning behind this behaviour needs to be further explored.

Figure 8 shows the orbit for half-arc splitting to around 40 sections, which corresponds to approximately fifteen B1, fourteen B1S, and six B1L dipoles per subfamily. As expected, with less splitting the orbit becomes larger, with an amplitude of around 100 microns. The relative beta function and dispersion for this case are shown in Figure 9 and Figure 10. It can be seen that as compared to the 50 micron case, the dispersion is increased tenfold and beta function twofold, which is already a significant deterioration. Additionally, previously observed periodicity of deterioration is still existent.

Figure 11 shows the orbit for half-arc splitting to around 10 sections, which corresponds to approximately sixty B1, fifty five B1S, and twenty B1L dipoles per subfamily. It can be seen that for the amplitude of around 200 microns, the orbit changes quite a lot, with features of grouping blocks. The relative beta function and dispersion for this case are shown in Figure 12 and Figure 13. Once again, as compared to the 100 micron case, the dispersion is increased twofold and beta function tenfold. However, when compared to the perfect tapering, it is evident that the deterioration of optics has become tremendous. The results from this most extreme case strongly imply the need for optics rematching and some form of dispersion correction, which would necessarily be the next step for the average tapering study.

	N			$\epsilon_x[1e^{-10}]$		$\frac{\Delta\beta}{\beta^{Ref}}[1e^{-3}]$		$\Delta\eta_x[1e^{-4}]$	
	B1	B1S	B1L	Average	Individual	IP1	IP2	IP1	IP2
50 μm	6	5	2	5.583	6.295	4.7243	3.7244	1.39	1.35
100 μm	16	14	6	9.547	6.295	9.61	9.62	0.525	0.656
200 μm	63	58	25	6.348	6.295	16.52	16.51	6.15	6.17

Table 2: Results of average tapering where: N is the number of dipoles per subfamily, ϵ_x is the emittance in the x plane for perfect and average tapering, $\frac{\Delta\beta}{\beta^{Ref}}$ is the relative beta function at IP1 and IP2, and $\Delta\eta_x$ is the absolute dispersion in x plane at IP1 and IP2.

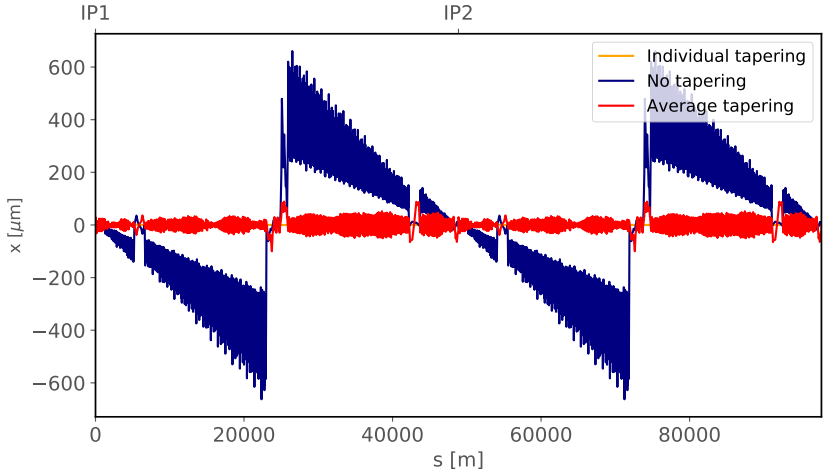

Figure 5: Beam orbit of 50 micron after average tapering is shown in red.

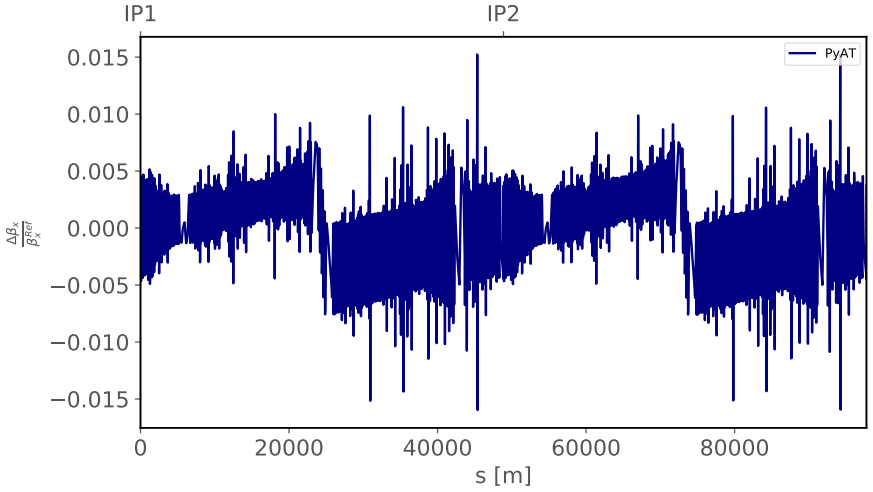

Figure 6: Relative beta function, as compared to no tapering case, for 50 micron orbit.

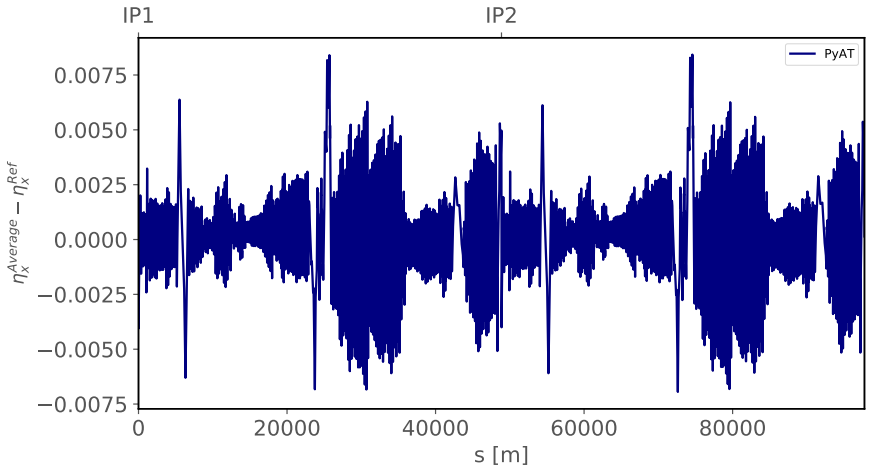

Figure 7: Relative dispersion, as compared to no tapering case, for 50 micron orbit.

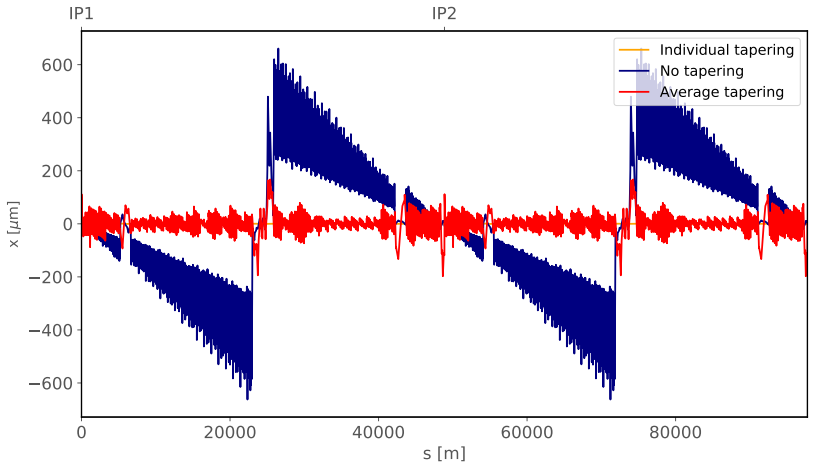

Figure 8: Beam orbit of 100 micron after average tapering is shown in red.

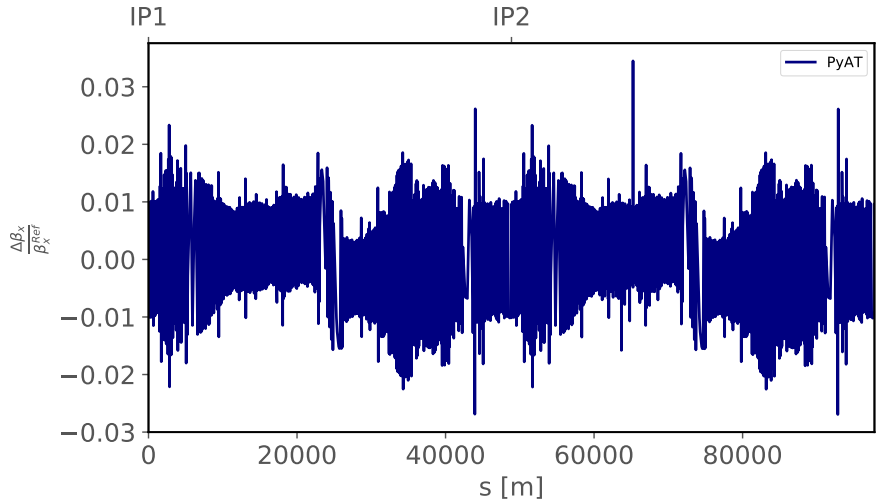

Figure 9: Relative beta function, as compared to no tapering case, for 100 micron orbit.

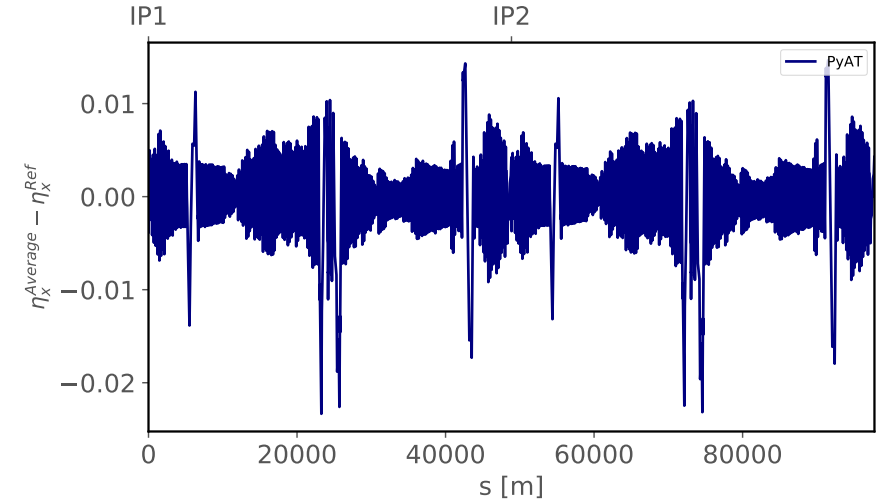

Figure 10: Relative dispersion, as compared to no tapering case, for 100 micron orbit.

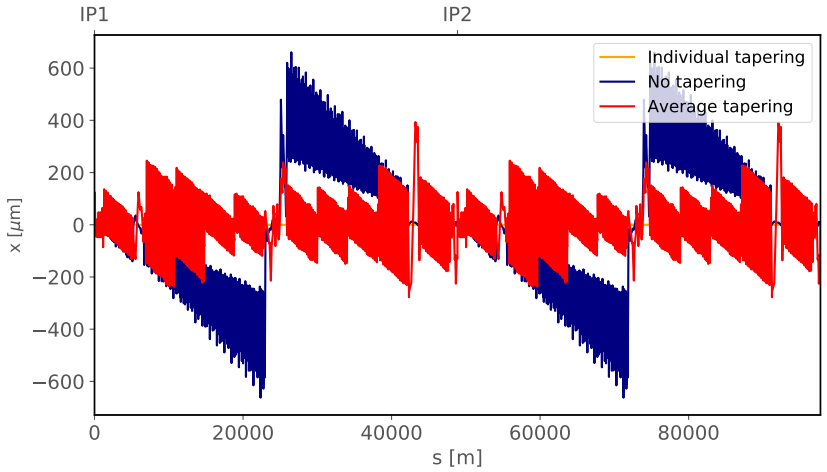

Figure 11: Beam orbit of 200 micron after average tapering is shown in red.

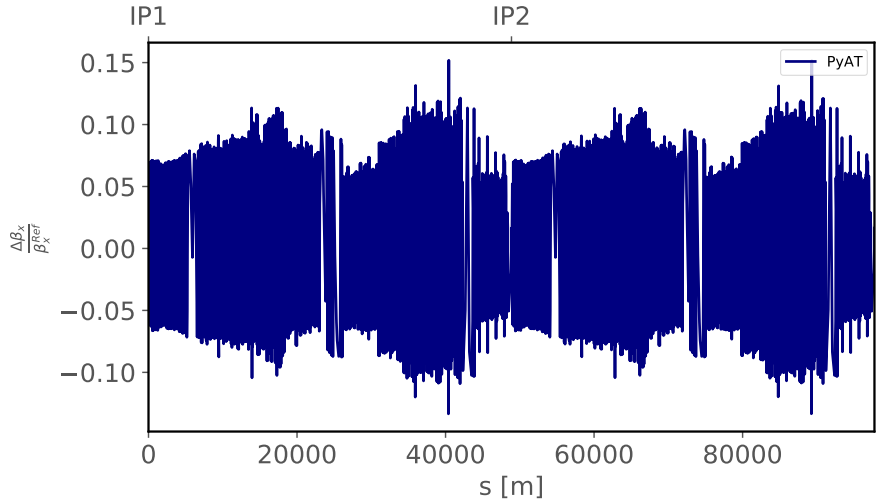

Figure 12: Relative beta function, as compared to no tapering case, for 200 micron orbit.

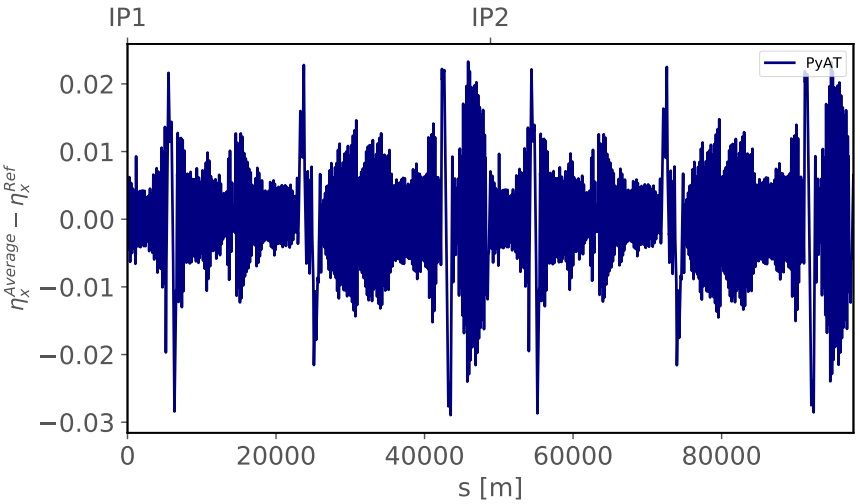

Figure 13: Relative dispersion, as compared to no tapering case, for 200 micron orbit.

4 Conclusion

Tapering schemes are very important in the context of future circular lepton colliders. Due to synchrotron radiation losses the particles are experiencing orbit changes, and besides needing to resupply them with energy using RF fields, there is also a need to adjust their sawtooth-orbit using tapering schemes. While the individual tapering scheme is most precise and is sure to give good orbit correction, it is also very costly for large scale rings, as it requires individual power supplies for each magnet. This is the reason why in this paper a prototype average tapering scheme for the Higgs lattice has been shown.

In order to simulate alternative tapering for the FCC-ee lattice, python implementation of the AT tools (pyAT) has been used. The first benchmarking of pyAT optics calculation with synchrotron radiation is shown. Dipole family selection and grouping modules were set, and first form of simplified tapering was explored. Moreover, besides the development of simplified tapering schemes, first tapering with pyAT is demonstrated.

The results obtained from simulations show that simplified tapering schemes leading to maximum orbit deviations of 50 and 100 microns are feasible. However, increasing the number of dipoles per power supply clearly shows a deterioration of both the orbit and optics functions. Furthermore, it has been observed that the optics deterioration shows periodic behaviour every half accelerator length and peculiar deviations for 100 micron orbit which may be due to the breaking of sextupole pair symmetry. These results indicate that further rematching of the optics will be critical for tapering schemes with larger orbit deviation tolerances.

Following the further investigation of the proposed form of simplified tapering, would it prove as a feasible solution for the Higgs lattice - which the results shown in this paper strongly suggest, only the top energy lattice would need perfect tapering. This prospect makes it very interesting for future studies.

References

Härer, Bastian, Andreas Doblhammer, and Bernhard Holzer. "Tapering Options and Emittance Fine Tuning for the FCC-ee Collider." In *7th International Particle Accelerator Conference*. June 2016. https://doi.org/10.18429/JACoW-IPAC2016-THPOR003.